IOPscience

OPEN ACCESS

Gas Evolution in Inner Disk Cavities from a Synergic Analysis of IR-CO and UV-H_2 Spectra

Michael A. Sánchez[1], Andrea Banzatti[1], Keri Hoadley[2], Kevin France[3], and Simon Bruderer[4]

Research Notes of the AAS, Volume 5, Number 4

Focus on AAS 237

Citation Michael A. Sánchez *et al* 2021 *Res. Notes AAS* **5** 78

banzatti@txstate.edu
banzatti@txstate.edu
[1] Department of Physics, Texas State University, San Marcos, TX, USA; banzatti@txstate.edu

[2] California Institute of Technology, Pasadena, CA, USA

[3] Astrophysical & Planetary Sciences, University of Colorado, Boulder, CO, USA

[4] Max-Planck-Institut fur Extraterrestrische Physik, Garching, Germany

Andrea Banzatti https://orcid.org/0000-0003-4335-0900

Keri Hoadley https://orcid.org/0000-0002-8636-3309

Kevin France https://orcid.org/0000-0002-1002-3674

Received March 2021
Accepted April 2021
Published April 2021

https://doi.org/10.3847/2515-5172/abf43c

Protoplanetary disks; Molecular spectroscopy; Exoplanet formation; Circumstellar disks; Near infrared astronomy; Ultraviolet astronomy; Molecular gas; Pre-main sequence stars

Abstract

We are conducting a multi-wavelength analysis of high-resolution molecular spectra that probe the evolution of gas in the inner 10 au in protoplanetary disks. A sample of 15 disks has been combined to probe a range of inner disk structures including small and large dust cavities. Half of the sample has been observed in far-ultraviolet H_2 emission with a new HST-COS program (GO-14703), that we have combined to near-infrared spectra of CO emission as observed with VLT-CRIRES and IRTF-iSHELL. This synergic dataset traces the evolution and depletion of CO and H_2 in inner disk cavities and shows an evolving radial stratification of the molecular gas, where CO lines are narrower than H_2 lines in disks with cavities. CO rotation diagrams also show significant evolution, suggesting a change in gas excitation as CO emission recedes to larger disk radii.

1. Introduction

While ALMA observations reveal protoplanetary disk structures at >10 au in great detail (e.g. Andrews 2020), the best probe of inner disk gas at <10 au is high resolution spectroscopy at infrared (IR) and ultraviolet (UV) wavelengths. Warm ($T > 500$ K) H_2 can be observed at near- and mid-infrared wavelengths using ground-based spectrographs, with low detection rates (Bitner et al. 2008; Gangi et al. 2020). Hot ($T > 1500$ K) H_2 has been observed in a sample of ~30 disks in the far-ultraviolet using the COS and STIS spectrographs on the Hubble Space Telescope (France et al. 2012; Hoadley et al. 2015). The CO molecule is less abundant than H_2 by $\sim 10^4$, but it is an extremely effective tracer of gas in disks. Rovibrational CO spectra at NIR wavelengths probe gas at temperatures of ~300–1500 K and have been observed in hundreds of disks with a suite of spectrographs (e.g. Najita et al. 2003; Brittain et al. 2007; Pontoppidan et al. 2011; Salyk et al. 2011; Brown et al. 2013; Banzatti et al. 2018). Both IR-CO and UV-H_2 spectra have been identified as tracers of inner disk evolution, where emission line profiles shrink in velocity (i.e., reflecting a lower Keplerian velocity at larger disk radii) with the depletion of inner disk dust (Banzatti & Pontoppidan 2015; Hoadley et al. 2015).

The relative distribution of H_2 and CO in the inner dust cavity of one disk, RY Lup, has been studied in Arulanantham et al. (2018). In this work, we combine for the first time these molecular tracers for a sample of 15 protoplanetary disks spanning a range in evolutionary phases. The ultimate goal of this program is to study inner disk evolution to test models of planet formation and wind dispersal (e.g. Ercolano & Pascucci 2017).

2. Sample and Data

The sample includes 15 disks around T Tauri and Herbig stars, which were selected from previous works to trace a range of phases in inner disk depletion from dust and gas (AA Tau, CV Cha, DF Tau, DoAr 44, DR Tau, EX Lup, RU Lup, RY Lup, TW Cha, TW Hya, HD 135344B, HD 144432, HD 142527, MWC 758, HD 139614). The H_2 spectra for this sample come from France et al. (2012), Hoadley et al. (2015), and a new HST-COS program (GO-14703, PI: Banzatti) that was requested for this analysis (providing half of the sample). The CO spectra come from Pontoppidan et al. (2011), using VLT-CRIRES (Kaeufl et al. 2004), and Banzatti et al. (2018), using IRTF-iSHELL (Rayner et al. 2016).

Figure 1 illustrates the two molecular lines in each disk, scaled in flux and shifted in velocity to focus the comparison on their widths. The H_2 line profiles are stacks of lines in the [1, 4] progression, from K. Hoadley et al. (2021, in preparation). The CO line profiles are stacks of $v = 1 - 0$ lines from Banzatti & Pontoppidan (2015), Banzatti et al. (2018). The sample is ordered by the infrared index n_{13-30}, which is sensitive to the formation and size of inner disk dust cavities (Banzatti et al. 2020): disks with $n_{13-30} < 0$ are "full" disks (half of this sample), those with $n_{13-30} > 0$ have an inner disk dust cavity (the other half of the sample). The lower-left plot in Figure 1 shows the ratio of H_2 to CO full-width-at-half-maximum (FWHM) as a function of n_{13-30}, to analyze a trend that is visible in the line profiles: full disks have similar H_2 and CO line widths, suggesting a similar radial distribution, while cavity disks have CO lines narrower than H_2, implying that CO is depleted in an inner disk region where H_2 still survives. The data are significantly correlated, with a Pearson coefficient of 0.62 (p-value of 0.02). Two of the full disks, DR Tau and RU Lup, appear as outliers, with CO lines narrower than H_2 lines; these stars are known to have outflows and might have some low-velocity CO emission from an inner disk wind (Pontoppidan et al. 2011).

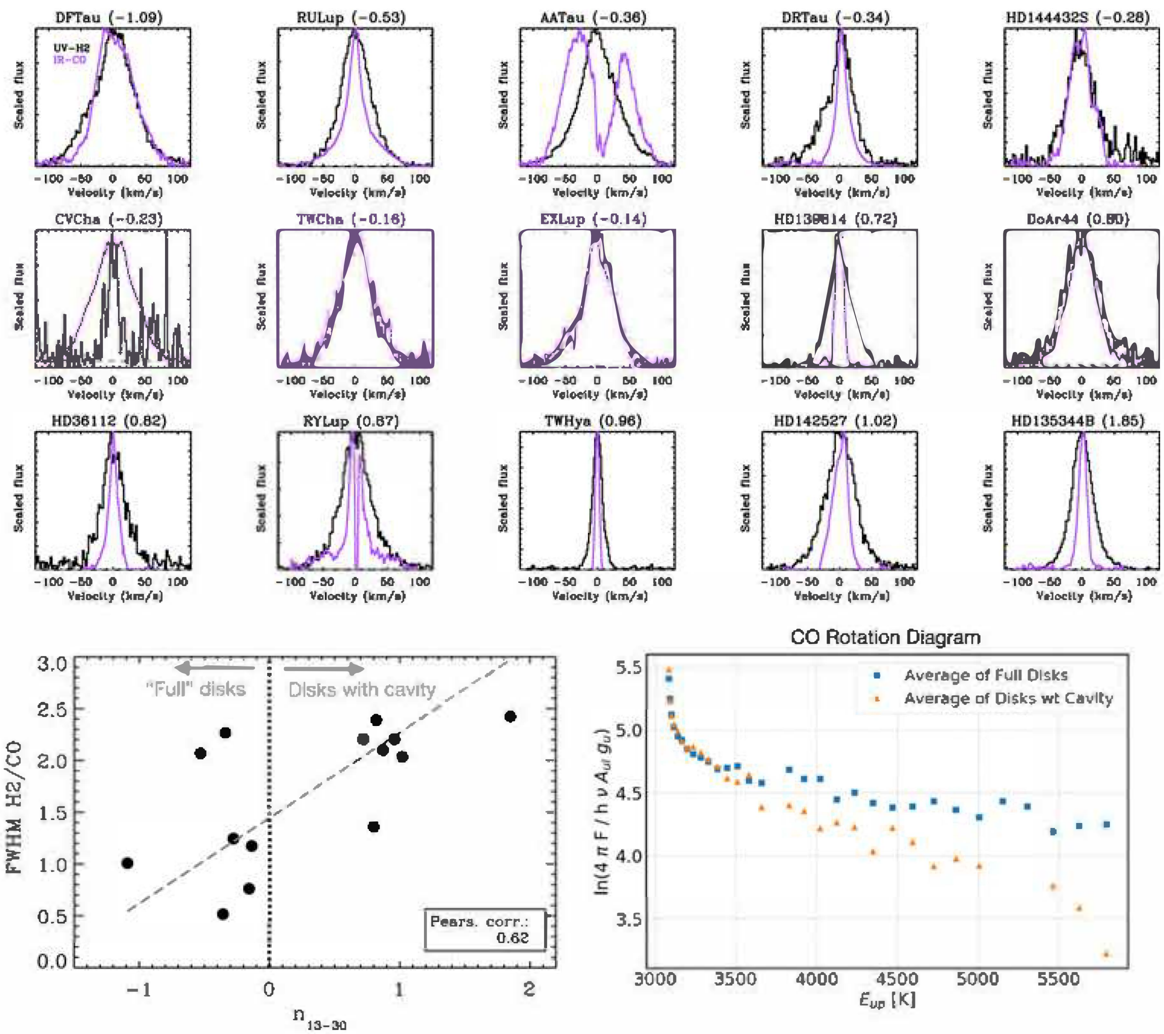

Figure 1. *Top*: comparison of CO (purple) and H_2 (black) line profiles for the whole sample, ordered by the infrared index n_{13-30} (reported next to each target name). *Bottom left*: the ratio of H_2 to CO lines FWHM as a function of n_{13-30}. A linear fit is shown with a dashed gray line, highlighting a trend that is already visible in the CO and H_2 line profiles, where CO lines are narrower than H_2 in disks with a cavity. *Bottom right*: CO rotation diagram for full and cavity disks.

3. Results and Discussion

The empirical difference in H_2 and CO line profiles between full disks and disks with cavities (Section 2) is accompanied by a significant difference in CO excitation. We construct rotation diagrams from the available CO $v = 1 - 0$ emission lines observed in each disk. Apart from a vertical shift, which can be given by different emitting areas, the shape of rotation diagrams match very well in each disk group according to their negative or positive infrared index n_{13-30}. We therefore average them in their respective group, and show these averages in Figure 1 (bottom right).

At upper level energies $E_{up} \gtrsim 3500$ K, the two average curves diverge, with cavity disks having a steeper slope than full disks. This difference can be interpreted as colder emission in disks with an inner cavity, although non-LTE excitation can also mimic similar effects (Goldsmith & Langer 1999). While their interpretation is still open, we conclude that strong empirical trends are visible in the data where as disks develop inner dust cavities, CO gas recedes to larger disk radii as compared to H_2, and CO excitation changes either in temperature or in departure from LTE. Future modeling of these combined spectral data sets promises to reveal key aspects of the physical and chemical evolution of inner disk molecular gas at the time of planet formation.

This work includes observations from the NASA/ESA Hubble Space Telescope. Support for Program GO-14703 was provided through a grant from the STScI under NASA contract NAS5-26555.

This work includes data taken with CRIRES at the VLT under program 179.C-0151 (PI K.Pontoppidan), and data taken with iSHELL at the IRTF under program 2016B049 (PI: A.Banzatti). We thank John Rayner for assistance with the iSHELL observations.

↑ Andrews S. M. 2020 *ARA&A* **58** 483
Crossref Google Scholar

↑ Arulanantham N., France K., Hoadley K. *et al* 2018 *ApJ* **855** 98
Crossref Google Scholar

↑ Banzatti A., Garufi A., Kama M. *et al* 2018 *A&A* **609** L2
Crossref Google Scholar

↑ Banzatti A., Pascucci I., Bosman A. D. *et al* 2020 *ApJ* **903** 124
Crossref Google Scholar

↑ Banzatti A. and Pontoppidan K. M. 2015 *ApJ* **809** 167
Crossref Google Scholar

↑ Bitner M. A., Richter M. J., Lacy J. H. *et al* 2008 *ApJ* **688** 1326
Crossref Google Scholar

↑ Brittain S., Rettig T. W., Simon T. *et al* 2007 *ApJL* **670** L29
Crossref Google Scholar

↑ Brown J. M., Pontoppidan K. M., van Dishoeck E. F. *et al* 2013 *ApJ* **770** 94
Crossref Google Scholar

↑ Ercolano B. and Pascucci I. 2017 *RSOS* **4** 170114
Crossref Google Scholar

↑ France K., Schindhelm E., Herczeg G. J. *et al* 2012 *ApJ* **756** 171
Crossref Google Scholar

↑ Gangi M., Nisini B., Antoniucci S. *et al* 2020 *A&A* **643** A32
Crossref Google Scholar

↑ Goldsmith P. F. and Langer W. D. 1999 *ApJ* **517** 209
Crossref Google Scholar

↑ Hoadley K., France K., Alexander R. D., McJunkin M. and Schneider P. C. 2015 *ApJ* **812** 41
Crossref Google Scholar

↑ Kaeufl H.-U., Ballester P., Biereichel P. *et al* 2004 *Proc. SPIE* **5492** 1218
ADS Google Scholar

↑ Najita J., Carr J. S. and Mathieu R. D. 2003 *ApJ* **589** 931
Crossref Google Scholar

↑ Pontoppidan K. M., Blake G. A. and Smette A. 2011 *ApJ* **733** 84
Crossref Google Scholar

↑ Rayner J., Tokunaga A., Jaffe D. *et al* 2016 *Proc. SPIE* **9908** 990884
Google Scholar

↑ Salyk C., Blake G. A., Boogert A. C. A. and Brown J. M. 2011 *ApJ* **743** 112
Crossref Google Scholar